Journal of Molecular Liquids 204 (2015) 44–49

Contents lists available at ScienceDirect

Journal of Molecular Liquids

journal homepage: www.elsevier.com/locate/molliq

Raman spectroscopy of micellization-induced liquid–liquid fluctuations in sodium dodecyl sulfate aqueous solutions

Tatiana A. Dolenko [a,*], Sergey A. Burikov [a], Sergey A. Dolenko [b], Alexander O. Efitorov [a,b], Yuriy A. Mirgorod [c]

[a] Physical Department, M.V. Lomonosov Moscow State University, 1 Bldg. 2, Leninskie Gory, Moscow 119991, Russia
[b] D.V. Skobeltsyn Institute of Nuclear Physics, M.V. Lomonosov Moscow State University, 1 Bldg. 2, Leninskie Gory, Moscow 119991, Russia
[c] Southwest State University, 94, 50th Anniversary of October St., Kursk 305040, Russia

ARTICLE INFO

Article history:
Received 26 May 2014
Received in revised form 12 January 2015
Accepted 13 January 2015
Available online 14 January 2015

Keywords:
Micellization
LDL-rich and HDL-rich clusters
Raman scattering
Multivariate curve resolution

ABSTRACT

This study is devoted to the investigation of the influence of micellization on structure properties of water and to micellization-induced liquid–liquid fluctuations in sodium dodecyl sulfate aqueous solutions. The dependence of Raman spectra of SDS aqueous solutions on surfactant concentration has been studied. Significant changes in the dependences of water valence band characteristics at the moment of micellization have been observed. Precision analysis of valence bands with the multivariate curve resolution–alternating least squares (MCR–ALS) method has confirmed these results. The observed structural changes in water are interpreted as significant fluctuations of the sizes of populations of LDL-rich and HDL-rich clusters of water.

1. Introduction

Amphiphilic substances play an important role in the processes of life activity of biological systems, and they find wide practical applications in technology processes [1–4]. Micelles are widely used for concentration and separation of metals [5], surfactants [6], and biologically active substances [7]. Overall interactions determining collective behavior of amphiphilic molecules in solutions play an important role in the formation of the structure of high-molecular compounds forming living organisms: proteins, nucleic acids, polysaccharides etc. [8,9]. Recently, the interest in micellar solutions of amphiphilic compounds rose due to the opportunity of using micelles as reactors for the synthesis of nanoparticles of metals and their compounds with fundamentally new properties [10], and also the opportunity of using micelles as components of agents for drug transport in bionanomedicine [11].

Dissolution of amphiphilic molecules in water is accompanied by a complex of interesting physico-chemical phenomena [12]. At low concentrations, the solution behaves as a usual strong electrolyte. When some specific concentration (critical concentration of micellization) is reached, the system undergoes a self-organization process — formation of micelles consisting of tens, hundreds or thousands of molecules. With further increase of concentration of amphiphilic molecules, the micelles undergo various transformations of their shape, sizes, and properties. The process of self-organization of the system is not finished when the limit of solubility of surfactants in water is reached. Above the solubility limit the system turns anisotropic and transfers to different liquid crystal phases [1,3].

At present there is no generally recognized theory describing the self-organization process [3]. The models used in practice often allow one to explain a number of properties and effects observed experimentally, but they are not universal, and they are unable to cover the whole diversity of the phenomena taking place in the system. It is considered that the surfactant sodium dodecyl sulfate (SDS, $C_{12}H_{25}SO_4Na$) is the most studied amphiphilic substance [3]. However, even sizes and composition of aqueous SDS micelles are still not determined explicitly. Different methods determine different sizes of micelles (see Table 1). Static methods of SAXS and SANS show that micelles consist of 60–70 molecules [13], while dynamic methods of nuclear magnetic resonance (NMR), dynamic light scattering (DLS) determine approximately 2 times less molecules [14]. While micellization of SDS is well explained by the phenomenological theory of hydrophobic interactions [3], the kinetics of micelle formation has many problems with explanation of experimental results [15]. Even the thermodynamics of formation of micellar systems is not developed completely.

It should be noted that a very important point in the investigation of the solutions of amphiphilic compounds is the study of the influence of micellization on the structure of the solvent. This is even more so if the solvent is water, whose properties and structure still remain far from being understood. With perfection of the equipment and methods of investigation, completely new and unexpected properties of water are revealed. Numerous theoretical and experimental studies of water properties show that in the scale of ≈1 nm there are clusters of low

* Corresponding author.
E-mail address: tdolenko@lid.phys.msu.ru (T.A. Dolenko).

http://dx.doi.org/10.1016/j.molliq.2015.01.021
0167-7322/

Table 1
Measured values of critical concentration of submicellization (CCSM) and critical micelle concentration (CMC) of sodium SDS in water.

Method of determination	CCSM, M	CMC, M
Fluorescence		$7.4 \cdot 10^{-3}$ [48], $8.0 \cdot 10^{-3}$ [49]
Surface tension, conductance		$8.0 \cdot 10^{-3}$ [32], $7.2 \cdot 10^{-3}$ [50]
Conductance		$8 \cdot 10^{-3}$ [48], $5.5 \cdot 10^{-3}$ [48], $6.7 \cdot 10^{-4}$ [51]
Benzoylacetone (BZA)-abs.		$7.8 \cdot 10^{-3}$ [48]
(BZA)-abs.		$2.8 \cdot 10^{-3}$ [48]
Resonance Rayleigh scattering	$1.4 \cdot 10^{-4}$ [32]	$8.0 \cdot 10^{-3}$ [32]
Isothermal compressibility	$3.0 \cdot 10^{-4}$ [47]	
Viscosity	$3.5 \cdot 10^{-4}$ [47]	
Shift of water band (5181 cm^{-1})	$3.2 \cdot 10^{-4}$ [47]	
Activity coefficient	$7.3 \cdot 10^{-4}$ [52]	
Raman spectroscopy	$6.0 \cdot 10^{-4}$, present work	$6.0 \cdot 10^{-3}$, present work

density liquid (LDL) and high density liquid (HDL), and phase LL-transition (liquid–liquid transition) between them can take place in the supercooled region [16–20]. Hypothesis of existence of the second critical point in water is under general discussion in literature now. Calculations show that the hypothetic "second" critical point of LL-transition in water is located in the region of the pressure–temperature phase diagram known as "no man's land" at temperature below the homogeneous nucleation temperature $T < T_H = 235$ K [16–20]. In many publications, theoretical and experimental evidence of possible existence of LL-transition in water and in aqueous solutions in supercooled state is presented [16–18,21]. Since experimental study of liquids in supercritical states is almost an impossible task, it is very hard to get convincing evidence of existence of phase LL transition in water. Nevertheless, many researchers try to obtain experimental verification of coexistence of LDL and HDL clusters in supercooled water and aqueous solutions. For example, the authors of [22] discovered the change of ratio of LDL and HDL clusters in water in the temperature range from 183 K up to 273 K by temperature dependences of half width and of integral intensities of the components of valence and bending bands of FTIR spectra of water. Experimentally, Mishima [23] found polyamorphic phase separation in water/LiCl solutions: an LL-transition of water itself induces phase separation between LDL with less solute and HDL with more solute. This finding is also supported by recent numerical simulations [24].

An active discussion about existence of water inhomogeneity on the nanometer-length scale at ambient conditions was opened in literature [25–29]. Wikfeldt et al. [25–27] have performed theoretical calculation and experimental demonstration of existence of density fluctuations in water at ambient conditions at 1 nm scale by the method of small-angle X-ray scattering (SAXS). Basing on SAXS data and X-ray Raman spectroscopy (using synchrotron radiation), the authors proposed that the density fluctuations were caused by difference between tetrahedral-bonded water molecules and molecules with broken hydrogen bonds, i.e., between low and high density water clusters. The authors of [28,29] claim that spectroscopic (Raman, IR, XAS, XES, etc.) data from water cannot be used to imply two-state behavior. Such debates are evidence of the fact that this problem is far from its solution.

In [30,31], the hypothesis that formation of micelles in aqueous solutions is accompanied by sharp fluctuations of concentrations of LDL and HDL clusters is set up. When amphiphiles are dissolved in water, hydrophobic hydration of hydrocarbon groups results in forming of a thin layer of water molecules around them, with a special near structure. In [30], this aggregate of water molecules, formed as the result of dissolving of an amphiphile, was called a nanocluster, or a small system. Nanoclusters are built into a continuous network of hydrogen bonds of water. They are stabilized by the hydrocarbon part of the molecule of amphiphile, and they have greater lifetime compared to other water clusters. At increasing concentration of amphiphiles, a transfer from hydrophobic hydration to hydrophobic interactions of hydrocarbon groups takes place. The concentration corresponding to this transition is called either critical concentration of submicellization (CCSM) [31] or critical premicelle concentration (CPC) [32].

The concentration, at which the ability of water network of hydrogen bonds to include amphiphilic molecules is exhausted, and they form micelles, is critical for the structure of the solution, and it is called critical micellization concentration (CMC). For aqueous solutions of SDS, the value of CMC equals $(8.0 \pm 0.2) \cdot 10^{-3}$ M [32]. At CMC, abrupt change of surface and volume properties of aqueous solutions (surface tension, electrical conductivity, light scattering etc.) occurs [2,4,33]. Micellization is accompanied both by sudden change of enthalpy (it characterizes first-order phase transitions) and by sudden change of isobaric heat capacity showing manifestation of second-order phase transition [2,4]. Thus, behavior of thermodynamic characteristics of aqueous solutions of amphiphiles at micellization can indicate possible significant structure changes in thin water layers around hydrocarbon groups of amphiphiles in concentration region of their aggregation, when their practically important properties become apparent — detergent effect, wetting, foam formation etc.

At present time, investigations of aqueous solutions of amphiphilic molecules are still topical, and they are conducted at the highest possible experimental level, including methods of vibrational spectroscopy [1,34–37]. However, nearly in all studies, Raman and IR spectroscopy are used to study the behavior of carbon tails of amphiphilic molecules in water, micelles, and in micelle associates by the behavior of vibrational bands of CH-groups. So, the authors of [34] studied the dependence of the intensity variations of both the symmetrical and antisymmetrical vibration modes of CH_2 groups situated in the region 2800–3000 cm^{-1} and of skeletal vibrations (C–C binding) in the region 1050–1150 cm^{-1} on concentrations of amphiphiles. Actively studied were the changes of conformational order of the SDS alkyl-chain at the air–solution interface and in the bulk with increasing SDS concentrations and temperature of solutions by IR bands of CH and CH_2 [36–38], and by the behavior of CH_2–CH_2 and CH_2–O IR bands [39]. The authors of [1] determine the state of alkyl chains of SDS in water by the ratio of intensities of the bands of asymmetric valence vibrations of methylene (2925 cm^{-1}) and methyl (2960 cm^{-1}). In [40], it has been demonstrated that the separation between the two peaks of the most intense band in the SDS spectrum – the SO_2 asymmetric vibrational feature (1219 and 1249 cm^{-1}) – is an indicative of the conformational structure of amphiphilic molecules.

In this paper, the results of studies with laser Raman spectroscopy of structural peculiarities of SDS solutions during micellization are presented. The changes of the band of valence vibrations of OH– groups in the concentration range from $1 \cdot 10^{-4}$ M to $3.5 \cdot 10^{-2}$ M have been studied. Significant changes of quantitative characteristics of water valence band at the moment of micellization have been observed. This was confirmed by the results of using the multivariate curve resolution method. The observed structural changes in water are interpreted as significant fluctuations of the size of populations of LDL and HDL clusters. A method of CCSM and CMC value estimation using concentration dependences of Raman spectra has been proposed.

2. Experimental

To prepare solutions, sodium SDS ($C_{12}H_{25}SO_4Na$) from "Sigma-Aldrich" and bidistilled water (specific electrical conductivity 0.1 μSm/cm, pH = 5.9) were used. Sodium SDS was re-crystallized from ethanol. This re-crystallization was essential for cleaning amphiphile from possible mixtures of dodecyl alcohol. This mixture can substantially influence the beginning of micellization. Since the presence of dodecyl alcohol causes appearance of minimum in isotherm of surface tension, the absence of this mixture was controlled by the absence of minimum in the pointed curve near CMC value of $8 \cdot 10^{-3}$ M.

The signal of Raman scattering was excited by radiation of an argon laser (wavelength 488 nm, power about 450 mW). Elastic scattering was suppressed by an edge filter (Semrock). Spectra were measured in the region 200–4000 cm^{-1} with the resolution of 2 cm^{-1}. The data acquisition system consisted of a monochromator (Acton, focus length 500 mm, grating 900 mm^{-1}) and a CCD camera (Jobin Yvon, model Synapse BIUV). The temperature of samples was stabilized at 22.0 ± 0.2 °C. The spectra were normalized to laser power and to accumulation time.

3. Results

3.1. Peculiarities of concentration dependencies of Raman spectra of SDS aqueous solutions during micellization

Raman spectra of aqueous SDS solutions were measured in the concentration range from $1 \cdot 10^{-4}$ M to $3.5 \cdot 10^{-2}$ M with an increment of $1 \cdot 10^{-4}$–$1.5 \cdot 10^{-3}$ M. In Fig. 1, the high-frequency region of Raman spectra of SDS aqueous solutions at different concentrations is presented. In the region 2800–3800 cm^{-1}, valence bands of CH– and OH– groups can be observed. The band of vibrations of CH– groups (2800–3000 cm^{-1}) includes several peaks corresponding to symmetric valence vibrations of CH groups in CH_2 (2860 cm^{-1}), symmetric valence vibrations (2930 cm^{-1}) and antisymmetric valence vibrations (2960 cm^{-1}) of CH groups in CH_3. As SDS concentration increases, the intensity of valence bands of CH groups increases, and their positions remain practically unchanged.

Under increase of SDS concentration, much more considerable changes are suffered by the band of valence vibrations of hydroxyl groups (3000–3800 cm^{-1}), since its shape and position are very sensitive to change of intra- and inter-molecular bonds in solutions, especially to the change of the network of hydrogen bonds [41–45]. Experimental dependencies of the shift of the position of maximum $\nu_{max}(C)$ of the valence band of OH– groups and of the change of its shape on SDS concentration in water were analyzed. As a parameter characterizing quantitative changes of the valence band of OH– groups, the parameter $\chi_{21} = I(\nu_2) / I(\nu_1)$ was used in this study. It equals the ratio of intensities of high- and low-frequency regions of water valence band [43–46]. To make calculations determinate, the frequencies ν_1 and ν_2 were selected as extremum points of the first derivative of the valence band: $\nu_1 = 3260$ cm^{-1} and $\nu_2 = 3414$ cm^{-1}.

According to the concepts about the nature of water Raman spectrum [42,45,46], the high-frequency region of the valence band near 3414 cm^{-1} (intensity $I(\nu_2)$) is caused by vibrations of hydroxyl groups with weak hydrogen bonds, and the low-frequency region near 3260 cm^{-1} (intensity $I(\nu_1)$) by vibrations of hydroxyl groups with strong hydrogen bonds. Therefore, the χ_{21} parameter characterizes the fraction of weakly bonded OH groups in the solution, in respect to strongly bounded OH groups. Hence, increase of parameter χ_{21} corresponds to weakening of the network of hydrogen bonds in water, and decrease of χ_{21} corresponds to strengthening of connectivity of molecules. These changes of parameter χ_{21} can also be interpreted from the point of view of equilibrium shift between LDL-rich and HDL-rich clusters [22]: increase of χ_{21} corresponds to increase of the HDL-rich cluster (loose structure) and decrease of χ_{21} signifies shift of equilibrium towards LDL-rich cluster (rigid structure).

Accuracy of determination of the position of maximum of valence band of OH– groups and accuracy of determination of parameter χ_{21} were evaluated statistically from a set of 18 water Raman spectra of the same sample. It turned out that the frequency of maximum could be determined with accuracy 2 cm^{-1}, and parameter χ_{21} — with accuracy 0.002.

As one can see from Fig. 2, experimental dependence of parameter χ_{21} on SDS concentration has the following peculiarities. Solvation of SDS in water up to concentration $6 \cdot 10^{-4}$ M practically does not change water structure. During further increase of SDS concentration from $6 \cdot 10^{-4}$ M up to $4 \cdot 10^{-3}$ M, the value of χ_{21} increases, and this indicates shift of the equilibrium towards HDL-rich clusters. At SDS concentrations greater than $4 \cdot 10^{-3}$ M, a stage of SDS molecule aggregation begins — appearance of spherical micelles. This process changes the structure of thin layer of water molecules around micelles significantly.

At a concentration range of $4 \cdot 10^{-3}$ M–$8 \cdot 10^{-3}$ M, significant decrease of parameter χ_{21} can be observed (i.e. step-wise formation of LDL-rich clusters). At further increase of concentration up to $1.5 \cdot 10^{-2}$ M, χ_{21} value significantly increases and then reaches plateau corresponding to value χ_{21} that is a little smaller than χ_{21} for pure water. Such behavior of χ_{21} dependence corresponds to backward shift of equilibrium — towards more loose HDL-rich cluster structure (i.e. to the

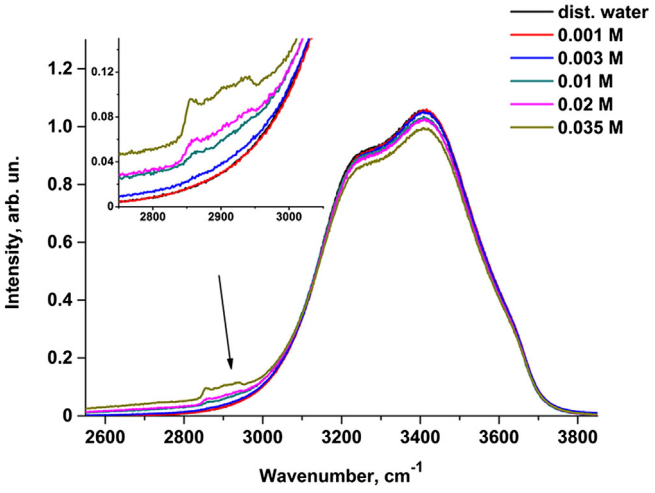

Fig. 1. High-frequency region of Raman spectra of SDS aqueous solutions at different concentrations.

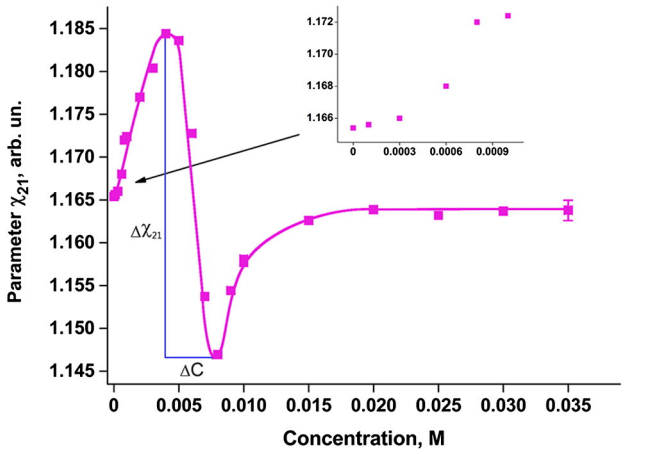

Fig. 2. Dependence of parameter χ_{21} on SDS concentration in water. Accuracy of determination of χ_{21} is 0.002. The inset shows the part of the curve in the concentration range from 0 to 0.001 M.

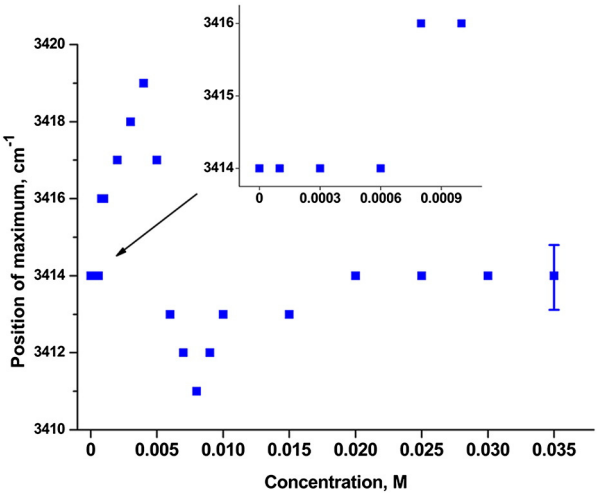

Fig. 3. Dependence of the position of maximum of the valence band of OH– groups on SDS concentration.

equilibrium of water clusters, which takes place in ordinary water). According to literature data [32,47–52], the concentrations of SDS, when peculiarities in the behavior of the dependence $\chi_{21}(C)$ (Fig. 2) can be observed, correspond to critical concentrations for aqueous solutions of SDS: $6 \cdot 10^{-4}$ M — CCSM, $6 \cdot 10^{-3}$ M (average concentration for the range $(4–8) \cdot 10^{-3}$ M) — CMC, see Table 1.

Similar behavior can be observed for the dependence $\nu_{max}(C)$ of the position of maximum of valence band of OH– groups on SDS concentration in the pointed range (Fig. 3). Reconstruction of water structure begins from SDS concentration $6 \cdot 10^{-4}$ M. Significant shift of maximum towards lower frequencies under increase of concentration from $4 \cdot 10^{-3}$ M up to $8 \cdot 10^{-3}$ M corresponds to essential strengthening of hydrogen bonds. Under further concentration change from $8 \cdot 10^{-3}$ M up to $1 \cdot 10^{-2}$ M, hydrogen bonds significantly weaken.

Step-wise changes of dependencies $\chi_{21}(C)$ and $\nu_{max}(C)$ in Figs. 2 and 3 near critical micelle concentration (CMC) of SDS can be explained by micellization-induced significant fluctuations of sizes of populations of LDL-rich and HDL-rich clusters in the layer of water molecules around micelles. According to Raman spectroscopy data (Fig. 2), the shift of equilibrium from water clusters with high density (HDL-rich clusters with weak hydrogen bonds) to water clusters with low density (LDL-rich clusters with strong hydrogen bonds) begins at SDS concentration $6 \cdot 10^{-4}$ M. This value is near to the average CCSM value $5.7 \cdot 10^{-4}$ M [47], but it is greater than the corresponding value measured by resonance Rayleigh spectroscopy ($1.2 \cdot 10^{-4}$ M) [32]. This implies that the beginning of the shift of equilibrium between LDL-rich and HDL-rich clusters depends on mixtures or on the structure of populations of water clusters.

3.2. Analysis of Raman spectra of SDS aqueous solutions using the MCR–ALS method

The multivariate methods are very powerful tools to resolve multicomponent mixture systems. Multivariate curve resolution (MCR) is a model-free or a soft-modeling chemometric method that focuses on describing the evolution of experimental multi-component measurements through their pure component contributions [53,54]. MCR–ALS is an algorithm that solves the MCR basic bilinear model using a constrained Alternating Least Squares algorithm.

The essence of the Multivariate Component Resolution method is the search for a decomposition of the experimental data matrix D (in our case, the array of Raman spectra of water solutions of SDS at different concentrations) into a matrix product of the matrix C of pure concentration profiles of different components and the transposed matrix S^T of pure spectra of different components:

$$D = CS^T + E. \quad (1)$$

Here E is the matrix of residuals which is minimized during the decomposition. Selection of one of the large number of possible decompositions is performed in the ALS (alternating least squares) algorithm by alternatingly determining one of the matrixes C and S from the other one and matrix D, applying non-negativity constraint (in some cases also unimodality and closure constraints [55]) for both the spectra and concentration profiles, until the minimum of the decomposition error is obtained. Use of only such very general and natural constraints ensures that the decomposition obtained does not depend on the will of the scientist but reveals the objective properties of the studied object.

MCR is a classical and, at the same time, a fully alive data analysis tool that is still in progress in terms of theoretical developments and new applications. It was shown that the MCR–ALS method can be successfully used for remote sensing hyperspectral image resolution purposes [56], for understanding spectroscopic data from monitoring chemical reactions processes [57], or for complete resolving of measured spectrophotometric data of tautomerization equilibria in aqueous micellar solutions [58]. The MCR–ALS method has been used to study molecular association in alcohol solutions [59–61]. Three-component and four-component MCR–ALS analysis has been used to resolve the Raman and IR spectra which are composed of overlapped bands, and to identify the composition of methanol and ethanol hydrates [59–61].

In our studies, the MCR–ALS method was used for analysis of water valence bands (3000–3700 cm^{-1}) of Raman spectra obtained in the concentration range from $1 \cdot 10^{-4}$ M up to $3.5 \cdot 10^{-2}$ M. The best accuracy was obtained by decomposition of water valence bands using MCR–ALS in the stated range of concentrations of SDS in the solutions into 2 components (Figs. 4, 5).

Calculation of χ_{21} for the resolved components demonstrated that for component 1, $\chi_{21} = 1.44$, for component 2, $\chi_{21} = 1.15$. Such values of χ_{21} indicate that component 1 represents the contribution to the intensity of the valence band of water molecules with weak hydrogen bonds — HDL-rich clusters, and component 2 is caused by vibrations of strongly bound water molecules — LDL-rich clusters. In this case, it follows from concentration profiles of these components (Fig. 6) that under change of concentration of SDS in the solution from $4 \cdot 10^{-3}$ M up to $6 \cdot 10^{-3}$ M, the concentration of LDL-rich clusters in water significantly increases, achieving its maximal value at $6 \cdot 10^{-3}$ M, and the concentration of HDL-rich clusters decreases sharply, achieving at $6 \cdot 10^{-3}$ M its minimal value. When SDS concentration changes from

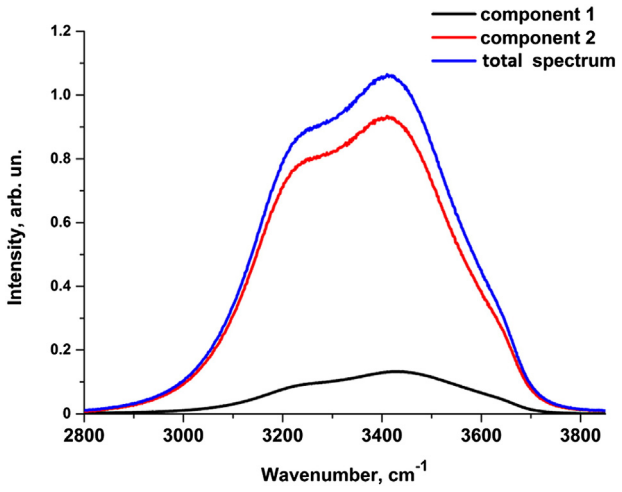

Fig. 4. Results of two-component MCR–ALS analysis of Raman valence bands of water in SDS solutions: Decomposition of water valence band by the MCR–ALS method.

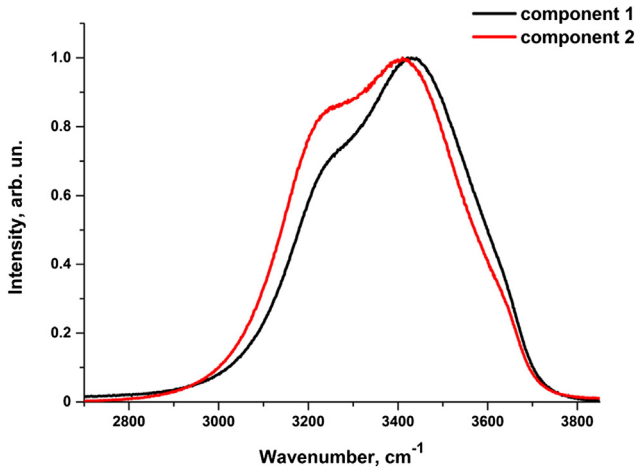

Fig. 5. Results of two-component MCR–ALS analysis of Raman valence bands of water in SDS solutions: Spectra of the resolved components (normalized by maximum intensity).

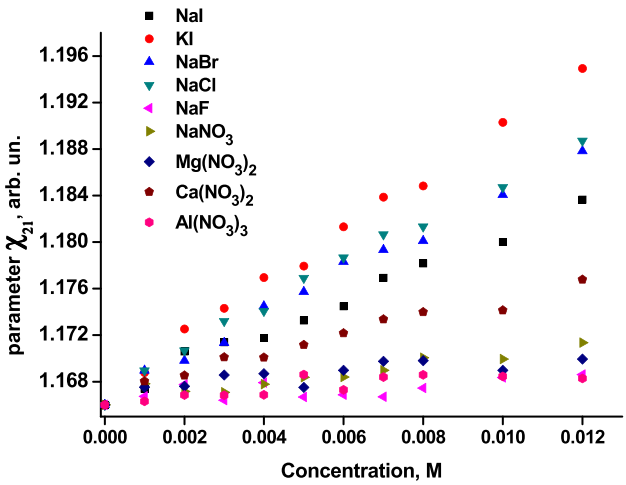

Fig. 7. The dependences of parameter χ_{21} of water Raman valence band on concentration of different salts in water.

$6 \cdot 10^{-3}$ M up to $8 \cdot 10^{-3}$ M, the fraction of LDL-rich clusters decreases, and the fraction of HDL-rich clusters increases. Near concentration of 0.05 M, the equilibrium between the populations of LDL-rich and HDL-rich clusters is settled. Similar behavior of the shift of equilibrium between LDL-rich and HDL-rich clusters was observed in the dependences χ_{21}(C) and ν_{max}(C) of valence bands (Figs. 2, 3) at the same SDS concentrations.

The obtained dependences of the characteristics of water valence bands and their components on SDS concentration in solutions (Figs. 2, 3) give quantitative evaluation of SDS CMC, equal to $6 \cdot 10^{-3}$ M (Table 1).

4. Discussion

We explain the significant changes of characteristics of water valence band in SDS solutions at CMC found in this study (Figs. 2, 3, 6) by specific influence of micellization on the structure of the hydration shell of a micelle.

When relatively simple salts are dissolved in water, the properties of the solvent, although perturbed, are still preserved. It follows from numerous literature data [41,42] and from our results obtained previously for solutions of inorganic salts [43,44]. In those papers, we studied the dependences of the same parameters of water Raman valence band as in the present article – of the parameter χ_{21} and the position of maximum of OH– groups Raman valence band – on concentration of inorganic salts. In Fig. 7 one can see the dependences of parameter χ_{21} of Raman valence band of OH– groups on concentration of different salts in water.

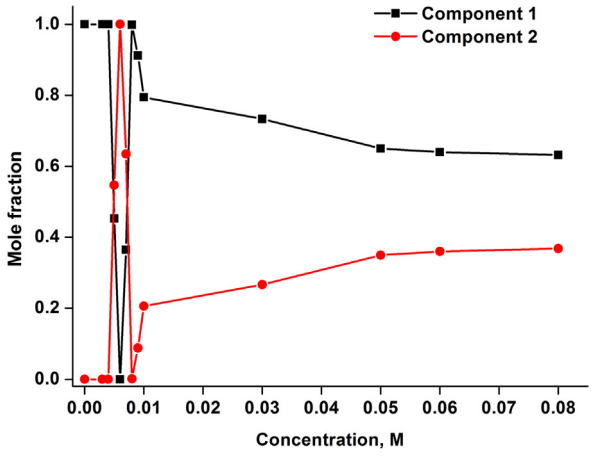

Fig. 6. Concentration profiles of the resolved components obtained by the MCR–ALS method.

As one can see from the dependences presented in Fig. 7, when inorganic salts are dissolved, the strength of hydrogen bonds in water changes smoothly without essential changes. We also obtained similar behavior of the studied parameters for water Raman valence bands in the solutions of ethanol, methanol, acetic acid etc. [60]. Moreover, we analyzed the concentration dependence of valence bands of OH– groups in water–ethanol solutions by the MCR–ALS method [62]. As can be seen in Fig. 7 from [62], concentration profiles of the resolved components obtained by the MCR–ALS method for water are smooth dependences on ethanol concentration, different from those for SDS solutions (Fig. 6).

As for spectral characteristics of SDS water solutions, we discovered significant changes in χ_{21}(C) and ν_{max}(C) dependences (Figs. 2 and 3 of the present article) in the concentration range where micellization takes place in the solution. Note that we talk about the micellization process, which proceeds very fast, and which still has much to learn about [3]. Until now, there is no detailed adequate description of physical and chemical processes taking place at the moment of micellization. All experimental studies of this process show that at the moment of micellization many thermodynamical parameters significantly change [1–3,12]. One of the possible explanations of the observed essential changes in the specified characteristics is the hypothesis of the shift of equilibrium between populations of HDL-rich and LDL-rich clusters.

5. Conclusions

By means of Raman spectroscopy using the MCR–ALS analysis it has been shown that micellization of SDS in water induces significant fluctuations of population sizes of LDL-rich and HDL-rich clusters. Significant shift of equilibrium from HDL-rich to LDL-rich in the populations of clusters occurs when SDS concentration changes from $4 \cdot 10^{-3}$ M to $6 \cdot 10^{-3}$ M, achieving maximum number of LDL-rich clusters at the concentration of $6 \cdot 10^{-3}$ M. At SDS concentration increasing from $6 \cdot 10^{-3}$ M to $8 \cdot 10^{-3}$ M, LDL-rich cluster fraction decreases, and HDL-rich cluster fraction grows. At the concentration of 0.05 M, the equilibrium between the numbers of LDL-rich and HDL-rich clusters is settled.

The suggested method for estimation of critical concentration of submicellization and of critical concentration of SDS micellization in water by concentration dependences of characteristics of water Raman valence band gives the values of CPMC and CMC that are in good agreement with literature data obtained with other methods.

Acknowledgment

This study was supported in part by Russian Foundation for Basic Research grant no. 14-02-00710-a.

References

[1] K.R. Lange, Surfactants: A Practical Handbook, Third ed. Hanser Gardner Pubns, Cincinnati, Ohio, 1999.
[2] J.N. Israelachvili, Intermolecular and Surface Forces, Second ed. Academic Press, London, 1992.
[3] R. Nagarajan, One hundred years of micelles: evolution of the theory of micellization, in: L. Romsted (Ed.), Surfactant Science and Technology: Retrospects and Prospects, Taylor and Francis, New York, 2013.
[4] A.I. Rusanov, Micellization in Aqueous Solutions of Surfactants, Khimiya, St. Petersburg, 1992.
[5] V.D. Karate, K.V. Marathe, Simultaneous removal of nickel and cobalt from aqueous stream by cross flow micellar enhanced ultrafiltration, J. Hazard. Mater. 157 (2008) 464–471.
[6] W.L. Hinze, E. Pramauro, A critical review of surfactant-mediated phase separations (cloud-point extractions): theory and applications, Crit. Rev. Anal. Chem. 24 (1993) 133–177.
[7] S.A. Basheer, M. Thenmozhi, Reverse micellar separation of lipases: a critical review, Int. J. Chem. Sci. 8 (2010) S57–S67.
[8] L.L. Vedenov, E.B. Levchenko, Supramolecular liquid crystalline structures in solutions of amphiphilic molecules, Sov. Phys. Usp. 141 (1983) 3–53.
[9] S. Terabe, Micellar electrokinetic chromatography for high-performance analytical separation, Chem. Rec. 8 (5) (2008) 291–301.
[10] W.L. Zhou, E.E. Carpenter, J. Lin, A. Kumbhar, J. Sims, C.J. O'Connor, Nanostructures of gold coated iron core–shell nanoparticles and the nanobands assembled under magnetic field, Eur. Phys. J. D 16 (2001) 289–292.
[11] G. Mao, C.R. Flach, R. Mendelsohn, R.M. Walters, Imaging the distribution of sodium dodecyl sulfate in skin by confocal Raman and infrared microspectroscopy, Pharm. Res. 29 (2012) 2189–2201.
[12] H. Wennerstrйom, B. Lindman, Micelles — physical-chemistry of surfactant association, Phys. Rep. Rev. Sec. Phys. Lett. 52 (1979) 1–56.
[13] B. Hammouda, Temperature effect on the nanostructure of SDS micelles in water, J. Res. Nat. Inst. Stand. Technol. 118 (2013) 151–167.
[14] H.-Un. Kim, K.-Hee Lim, Sizes and structures of micelles of cationic octadecyl trimethyl ammonium chloride and anionic ammonium dodecyl sulfate surfactants in aqueous solutions, Bull. Korean Chem. Soc. 25 (2004) 382–388.
[15] T. Toyota, K. Uchiyama, T. Kimura, T. Nomoto, M. Fujinami, Effects of surfactants and electrolytes on chemical oscillation at a water/nitrobenzene interface investigated by quasi-elastic laser scattering method, Anal. Sci. 29 (2013) 911–917.
[16] P.H. Poole, F. Sciortino, U. Essmann, H.E. Stanley, Phase behavior of metastable water, Nature 360 (1992) 324–328.
[17] C.A. Angell, Formation of glasses from liquids and biopolymers, Science 267 (1995) 1924–1935.
[18] O. Mishima, H.E. Stanley, Decompression-induced melting of ice IV and the liquid–liquid transition in water, Nature 392 (1998) 164–168.
[19] S. Harrington, R. Zhang, P.H. Poole, F. Sciortino, H.E. Stanley, Liquid–liquid phase transition: evidence from simulations, Phys. Rev. Lett. 78 (1997) 2409–2412.
[20] O. Mishima, H.E. Stanley, The relationship between liquid, supercooled and glassy water, Nature 396 (1998) 329–335.
[21] V. Holten, C.E. Bertrand, M.A. Anisimov, J.V. Sengers, Thermodynamics of supercooled water, J. Chem. Phys. 136 (2012) 094507.
[22] F. Mallamace, M. Broccio, C. Corsaro, A. Faraone, D. Majolino, V. Venuti, L. Liu, C.-Y. Mou, S.-H. Chen, Evidence of the existence of the low-density liquid phase in supercooled, confined water, Proc. Natl. Acad. Sci. U. S. A. 104 (2007) 424–428.
[23] O. Mishima, Phase separation in dilute LiCl–H_2O solution related to the polyamorphism of liquid water, J. Chem. Phys. 126 (2007) 244507.
[24] L. Le, V. Molinero, Nanophase segregation in supercooled aqueous solutions and their glasses driven by the polyamorphism of water, J. Phys. Chem. A 115 (2011) 5900–5907.
[25] C. Huang, T.M. Weiss, D. Nordlund, K.T. Wikfeldt, L.G.M. Pettersson, A. Nilsson, Increasing correlation length in bulk supercooled H_2O, D_2O, and NaCl solution determined from small angle X-Ray scattering, J. Chem. Phys. 133 (2010) 134504-1–134504-5.
[26] K.T. Wikfeldt, A. Nilsson, L.G.M. Pettersson, Spatially inhomogeneous bimodal inherent structure of simulated liquid water, Phys. Chem. Chem. Phys. 13 (2011) 19918–19924.
[27] C. Huang, K.T. Wikfeldt, T. Tokushima, D. Nordlund, Y. Harada, U. Bergmann, M. Niebuhr, T.M. Weiss, Y. Horikawa, M. Leetmaa, et al., The inhomogeneous structure of water at ambient conditions, Proc. Natl. Acad. Sci. U. S. A. 106 (2009) 15214–15218.
[28] A.K. Soper, J. Teixeira, T. Head-Gordon, Is ambient water inhomogeneous on the nanometer-length scale? Proc. Natl. Acad. Sci. U. S. A. 107 (2010) E44.
[29] A.K. Soper, Recent water myths, Pure Appl. Chem. 82 (2010) 1855–1867.
[30] Yu.A. Mirgorod, Thermodynamic analysis of the structure of aqueous solutions of C12–C18 hydrocarbons, J. Struct. Chem. 50 (2009) 456–460.
[31] Yu.A. Mirgorod, Cooperative self-organization in aqueous solutions, Russ. J. Gen. Chem. 64 (1994) 189–192.
[32] Y. Shi, H.Q. Luo, N.B. Li, Determination of the critical premicelle concentration, first critical micelle concentration and second critical micelle concentration of surfactants by resonance Rayleigh scattering method without any probe, Spectrochim. Acta A Mol. Biomol. Spectrosc. 78 (2011) 1403–1407.
[33] J.P. Marcolongo, M. Mirenda, Thermodynamics of sodium dodecyl sulfate (SDS) micellization: an undergraduate laboratory experiment, J. Chem. Educ. 88 (2011) 629–633.
[34] M. Picquart, Vibrational mode behavior of SDS aqueous solutions studied by Raman scattering, J. Phys. Chem. 90 (1986) 243–249.
[35] G. Cazzolli, S. Caponi, A. Defant, C.M.C. Gambi, S. Marchetti, M. Mattarelli, M. Montagna, B. Rossi, F. Rossi, G. Viliani, Aggregation processes in micellar solutions: a Raman study, J. Raman Spectrosc. 43 (2012) 1877–1883.
[36] T. Kawai, H. Kamio, T. Kondo, K. Kon-No, Effects of concentration and temperature on SDS monolayers at the air–solution interface studied by infrared external reflection spectroscopy, J. Phys. Chem. B 109 (2005) 4497–4500.
[37] R.B. Viana, A.B.F. da Silva, A.S. Pimentel, Infrared spectroscopy of anionic, cationic, and zwitterionic surfactants, Adv. Phys. Chem. 2012 (2012) 14 (Article ID 903272).
[38] F. Holler, J.B. Callis, Conformation of the hydrocarbon chains of sodium dodecyl sulfate molecules in micelles: an FTIR study, J. Phys. Chem. 93 (1989) 2053–2058.
[39] H. Okabayashi, M. Okuyama, T. Kitagawa, T. Miyazawa, The Raman spectra and molecular conformations of surfactants in aqueous solution and crystalline states, Bull. Chem. Sos. Jpn. 47 (1974) 1075–1077.
[40] T. Kawai, J. Umemura, T. Takenaka, Fourier-transform infrared study on the phase transitions of a sodium dodecyl sulfate-water system, Bull. Inst. Chem. Res. 61 (1983) 314–323 (Kyoto University).
[41] G.E. Walrafen, Raman spectral studies of water structure, J. Chem. Phys. 40 (1964) 3249–3256.
[42] M. Chaplin, Water structure and science, http://www.lsbu.ac.uk/water/2008.
[43] T.A. Gogolinskaia, S.V. Patsaeva, V.V. Fadeev, The regularities of change of the 3100–3700 cm^{-1} band of water Raman scattering in salt aqueous solutions, Dokl. Akad. Nauk SSSR 290 (1986) 1099–1103.
[44] S.A. Burikov, T.A. Dolenko, P.A. Velikotnyi, A.V. Sugonyaev, V.V. Fadeev, The effect of hydration of ions of inorganic salts on the shape of the Raman stretching band of water, Opt. Spectrosc. 98 (2005) 235–239.
[45] S.A. Burikov, T.A. Dolenko, V.V. Fadeev, I.I. Vlasov, Revelation of ions hydration in Raman scattering spectral bands of water, Laser Phys. 17 (2007) 1–7.
[46] T.A. Dolenko, S.A. Burikov, J.M. Rosenholm, O.A. Shenderova, I.I. Vlasov, Diamond–water coupling effects in Raman and photoluminescence of nanodiamond colloidal suspensions, J. Phys. Chem. C 116 (2012) 24314–24319.
[47] Yu.A. Mirgorod, Structure of dilute aqueous solutions of sodium dodecyl sulfate, J. Struct. Chem. 32 (1991) 853–856.
[48] A. Domínguez, A. Fernández, N. González, E. Iglesias, L. Montenegro, Determination of critical micelle concentration of some surfactants by three techniques, J. Chem. Educ. 74 (1997) 1227–1231.
[49] I. Casero, D. Sicilia, S. Rubio, D. Pérez-Bendito, Study of the formation of dye-induced premicellar aggregates and its application to the determination of quaternary ammonium surfactants, Talanta 45 (1997) 167–180.
[50] Y. Zimmels, I.J. Lin, Stepwise association properties of some surfactant aqueous solutions, Colloid Polym. Sci. 252 (1974) 594–612.
[51] S. Vijayan, D.R. Woods, H. Vaya, Bulk and interfacial physical properties of aqueous solutions of sodium lauryl sulphate and lauryl alcohol with air and benzene system. Part I. Aqueous solutions of sodium lauryl sulphate, Can. J. Chem. Eng. 55 (1977) 718–738.
[52] A.I. Rusanov, V.A. Prokhorov, Interphase Tensometry, Khimiya, St. Petersburg, 1994.
[53] R. Tauler, A. de Juan, Multivariate Curve Resolution–Alternating Least-Squares (MCR–ALS), MatLab Code, University of Barcelona, 1999.
[54] A. de Juan, R. Tauler, Multivariate curve resolution (MCR) from 2000: progress in concepts and applications, Crit. Rev. Anal. Chem. 36 (2006) 163–176.
[55] J. Saurina, S. Hernandez-Cassou, R. Tauler, Multivariate curve resolution applied to continuous-flow spectrophotometric titrations — reaction between amino-acids and 1,2-naphthoquinone-4-sulfonic acid, Anal. Chem. 67 (1995) 3722–3726.
[56] X. Zhang, R. Tauler, Application of multivariate curve resolution alternating least squares (MCR–ALS) to remote sensing hyperspectral imaging, Anal. Chim. Acta. 762 (2013) 25–38.
[57] M. Garrido, F.X. Rius, M.S. Larrechi, Multivariate curve resolution–alternating least squares (MCR–ALS) applied to spectroscopic data from monitoring chemical reactions processes, Anal. Bioanal. Chem. 390 (2008) 2059–2066.
[58] H. Abdollahi, V. Mahdavi, Tautomerization equilibria in aqueous micellar solutions: a spectrophotometric and factor-analytical study, Langmuir 23 (2007) 2362–2368.
[59] C.A. Holden, S.S. Hunnicutt, R. Sanchez-Ponce, J.M. Craig, S.C. Rutan, Study of complexation in methanol/water mixtures by infrared and Raman spectroscopy and multivariate curve resolution–alternating least-squares analysis, Appl. Spectrosc. 57 (2003) 483–490.
[60] S. Burikov, T. Dolenko, S. Patsaeva, Yu. Starokurov, V. Yuzhakov, Raman and IR spectroscopy research on hydrogen bonding in water–ethanol systems, Mol. Phys. 108 (2010) 2427–2436.
[61] S. Burikov, T. Dolenko, S. Dolenko, S. Patsaeva, V. Yuzhakov, Decomposition of water Raman stretching band with a combination of optimization methods, Mol. Phys. 108 (2010) 739–747.
[62] N. Hu, D. Wu, K. Cross, S. Burikov, T. Dolenko, S. Patsaeva, D.W. Schaefer, Structurability: a collective measure of the structural differences in vodkas, Agric. Food Chem. 58 (2010) 7394–7401.